Heat and Mass Transfer (2018) 54:3265–3274
https://doi.org/10.1007/s00231-018-2370-y

ORIGINAL

A comparison of the thermal and hydraulic performances between miniature pin fin heat sink and microchannel heat sink with zigzag flow channel together with using nanofluids

Weerapun Duangthongsuk[1,2] · Somchai Wongwises[2,3]

Received: 1 October 2017 / Accepted: 24 April 2018 / Published online: 4 May 2018

Abstract
In this study, a comparison of the convective heat transfer, pressure drop, and performance index characteristics of heat sinks with a miniature circular pin-fin inline arrangement (MCFHS) and a zigzag flow channel with single cross-cut structures (CCZ-HS) is presented. SiO_2-water nanofluids with different particle concentrations are used as the coolant. The effects of the heat sink type, particle concentration and fluid flow rate on the thermal and hydraulic performances are evaluated. The testing conditions are performed at the wall heat fluxes of 10 to 60 kW/m^2 and at a mass flow rate ranging from 0.18 to 0.6 kg/s. The dimension of heat sinks is equally designed at 28 × 33 mm. The heat transfer area of MCFHS and of CCZ-HS is 1430 and 1238 mm^2, respectively. Similarly, the hydraulic diameter of the flow channel of MCFHS and of CCZ-HS is 1.2 and 1.0 mm, respectively. The measured data indicate that the cooling performances of CCZ-HS are about 24–55% greater than that of MCFHS. The effects of the channel diameter and single cross-cut of the flow channel are more dominant than the effects of the fin structure and heat transfer area.

Keywords Nusselt number · Performance index · Pin fin · Microchannel · Nanofluid · Heat sink

Nomenclature

A	Area, m^2
C_p	Specific heat, J/kgK
d	Diameter, m
h	Heat transfer coefficient, W/m^2 °C
k	Thermal conductivity, W/m °C
L	Heat sink length, m
m	Mass flow rate, kg/s
Nu	Nusselt number
ΔP	Pressure drop, Pa
Q	Heat transfer rate, W
R	Thermal resistance, °C/W
Re	Reynolds number
T	Temperature, °C
t	Fin height, mm
V	Mean velocity, m/s
Q_v	Volume flow rate, m^3/s
W	Heat sink width, mm
$W_{p\,p}$	Pumping power, W

Greek symbols

ϕ	Volume fraction
ρ	Density, kg/m^3
μ	Viscosity, kg/ms
η	Performance index

Subscript

b	Bulk
ch	Channel
in	Inlet
out	Outlet
p	Particles
PF	Pin fin
nf	Nanofluid
S	Surface
th	Thermal
w	Water

✉ Somchai Wongwises
somchai.won@kmutt.ac.th

[1] Department of Mechanical Engineering, Faculty of Engineering, Southeast Asia University, Bangkok, Thailand

[2] Fluid Mechanics, Thermal Engineering and Multiphase Flow Research Lab. (FUTURE), Department of Mechanical Engineering, Faculty of Engineering, King Mongkut's University of Technology Thonburi, Bangmod, Bangkok, Thailand

[3] The Academy of Science, The Royal Institute of Thailand, Sanam Suea Pa, Dusit, Bangkok 10300, Thailand

1 Introduction

Heat sinks are one type of the heat transfer equipment normally used to transfer the heat generated by various electronic or mechanical devices using a working fluid medium, such as air or other liquid coolants. They are often used to dissipate heat from power semiconductor devices, high-voltage systems, the control units for medical equipment and locomotives, solar or wind power plants, and other electronic components. When the heat is dissipated from a device, an optimal temperature level of the system is obtained, which leads to improving the working performance, reliable functioning, and stability of the heat transfer system. Typically, two types of heat sinks exist: active and passive. For an active heat sink, an external power supply is required, such as an air-cooled and liquid-cooled one. For passive heat sinks, no extra mechanical components are needed. They are completely reliable and durable. Air is commonly used as a working medium. Focus on passive heat sinks, due to the thermal performance of liquids, is greater than the value of air or other gases. Heat sinks cooled by liquid can be made in a more compact manner and are especially more effective than their air-cooled counterparts. Moreover, among the many types of heat sinks available, heat sinks with a pin-fin structure have inherent advantages compared to plate-fin heat sinks due to the high heat transfer rate resulting from the redeveloping flow region [1], and the flow direction has no effect on the thermal performance.

Nowadays, modern electronic devices and heat transfer equipment are being rapidly developed and widely used. Microscale heat transfer devices are very popular and have become essential to use in many advanced applications. Due to the very small heat transfer area, the amount of heat generation is very high. Thus, proper cooling technology is required. More than a decade ago, many researchers studied the heat transfer performance and flow characteristic of the microscale heat transfer system. Understanding the heat transfer and fluid flow fundamentals of microscale heat transfer devices is necessary to achieve appropriate designs for practical applications. In addition to the optimum geometry of a heat sink, reducing the flow channel size and increasing the thermal performance of coolants should be done simultaneously to increase the heat dissipation rate. In 1981, Tuckerman and Pease [2] introduced the concept of the microchannel heat sink for enhancing heat transfer performance. Meanwhile, the concept of the nanofluid was first announced by Choi [3] in 1995. Both concepts related to heat transfer enhancement have attracted growing interest in recent years among a number of researchers. Thus, a heat sink with an optimum geometry and a very small flow channel using a high-thermal-performance fluid as the coolant is the most suitable tool for dissipating a high heat load generated from the advanced heat transfer device. Many research articles have reported a series of work regarding the abovementioned topic [4–6]. However, additional research activities in this field are amplified and described as follows:

In 2008, Kim et al. [7] presented a comparison of the thermal and friction characteristics of pin-fin and plate-fin heat sinks, experimentally. Their measured data indicated that, at a lower dimensionless pumping power, pin-fin heat sinks (PFHS) gave greater thermal resistances than did the plate-fin heat sinks. At a higher dimensionless pumping power, the contrary trend is observed. Yang and Peng [8] studied the thermal performance and fluid flow of a compound heat sink, such as a plate-fin heat sink and plate fins with some pins between the plates. The RNG $k-\varepsilon$ turbulence model is used to analyze the turbulent structure and behavior. The results indicated that the compound heat sink gave a greater thermal performance than did the plate-fin heat sink. Moreover, the compound heat sink with a plate fin and circular pins gave a greater performance than did the compound heat sink with a plate fin and square pins. The effect of cross-cuts on the heat transfer performances of heat sinks was experimentally examined by Kim and Kim in 2009 [9]. The results showed that the cross-cut heat sinks gave better thermal performances than did the plate-fin and square-pin fin heat sinks under a given pumping power. Teja and colleges [10] investigated the thermal and pressure drop performances of MCHS with different cross-sectional stacked shapes, such as a rectangular, triangular, pentagonal, and circular one. The CFD technique is used to analyze. However, the above literatures deal with single-phase fluid flows in several types of heat sinks.

For the use of nanofluids as coolants, the heat transfer and fluid flow in silicon MCHS was explored by Jang and Choi [11] numerically. The effects of the particle type, particle loading, and Reynolds number on the cooling performance were examined. The cooling performance of a nanofluid was greater than that of water by about 10%. Lee and Mudawar [12] reported the convective heat transfer performance of nanofluid flow in MCHS, experimentally. The results indicated that the heat transfer coefficient of a nanofluid is higher than that of a common fluid, especially at the entrance region of a heat sink. Bhattacharya et al. [13] presented the convective heat transfer coefficient of a nanofluid flowing through MCHS in a laminar flow regime, numerically. They stated that the heat transfer coefficient increased as the Reynolds number increased. Li and Kleinstreuer [14] conducted a study on the cooling performance of MCHS with a trapezoidal flow channel, numerically. The simulation results indicated that the use of nanofluids as coolants can intrinsically increase the thermal performance of MCHS compared to water. Ho et al. [15] studied the cooling performance of MCHS using nanofluids as coolants under a laminar flow regime, experimentally. Their data showed that the cooling performance of a nanofluid-cooled heat sink is 70% higher than that of a water-cooled heat sink, especially at a high flow rate. Nanofluids had no significant effect on pressure drop across the heat sink. Lelea [16] examined the local heat transfer coefficient and flow characteristic of Al_2O_3-water nanofluid flow in MCHS under a laminar flow regime, numerically. The simulation results demonstrated that, at a lower pumping power, heat transfer enhancement is high for the heating case. The vice-versa trend is obtained for the cooling case. The heat transfer and flow characteristics of nanofluids flowing through a microchannel heat exchanger (MCHE) with a square-shaped flow channel were evaluated by Mohammed and co-workers [17] numerically. Various types of nanofluids are used to verify the performance and flow under a laminar flow regime. The simulation results indicated that nanofluids gave greater thermal properties and greater heat transfer performances than did the common base fluid, with little penalty in the pressure drop. Selvakumar and Suresh [18] investigated the convective heat transfer performance of a copper heat sink cooled by nanofluids, experimentally. The convective heat transfer coefficient and pumping power of a nanofluid-cooled heat sink are about 30 and 15% higher than those of a heat sink cooled by water, respectively. The heat transfer of a 3-D MCHS using nanofluids as coolants was studied by Hung et al. [19] numerically. The nanoparticle type, particle size, particle volume fraction, base fluid, and pumping power affecting the thermal performance were considered. The simulation data illustrated that the thermal resistance of nanofluids decreases with increasing particle concentrations and then increases. Moreover, MCHS cooled by a nanofluid with smaller particle sizes gave better thermal performance than did MCHS cooled by a nanofluid with big particle sizes. For heat transfer enhancement, MCHS cooled by a nanofluid gave 21.6% greater thermal performance than did water-cooled MCHS. An experimental investigation on the heat transfer performance of nanofluid flow in MCHE was conducted by Putra et al. [20]. The effect of the nanofluid type, particle concentration, and Reynolds number on the heat transfer performance and fluid flow of MCHE was investigated under the laminar flow condition. The experimental results illustrated that the use of a nanofluid instead of a common base fluid could enhance the thermal performance of MCHE. The results also indicated that nanofluids gave better cooling performances than common pure water about 9% to 12%. Moreover, at particle concentration of 1.0 vol.%, a greater heat transfer coefficient was obtained for a SnO_2 nanoparticle compared to an Al_2O_3 nanoparticle. Moreover, at a lower particle concentration, a greater heat transfer coefficient is obtained for a CuO nanoparticle compared to an Al_2O_3 nanoparticle. Recently, Wu et al. [21] presented suitable criteria for using Al_2O_3-water nanofluids as coolants and flow in MCHS. This attempt was made to discover the most suitable working condition when applying Al_2O_3-water nanofluids to cool MCHS. As a result, they claimed that Al_2O_3-water nanofluids are not appropriate to use as coolants of MCHS. A heat transfer and friction factor of a cylindrical MCHS using a Cu-water nanofluid as a coolant was conducted experimentally by Azizi and colleges [22]. The measured data showed that the Nusselt number and friction factor of nanofluids were higher than those of water by about 43 and 45.5%, respectively. The thermal and hydraulic performances of MCFHS and CCZ-HS are described in the previous works of the authors [6, 23].

From the abovementioned data, many researchers reported that nanofluids exhibit dramatic heat transfer performances compared to common heat transfer fluids by several dozen percent, with little or no penalty in pumping power. Moreover, nanofluid-cooled MCHS also demonstrates superior cooling performance compared to MCHS cooled by water. This behavior is also found in miniature PFHS [4–6]. Furthermore, the straight flow channels of MCHS, such as those with circular, rectangular, triangular, and trapezoidal shapes, and PFHS are analyzed both experimentally and numerically. However, a comparison of the thermal performance, performance index (η), and flow characteristics between MCHS with a multiple-zigzag flow channel and single cross-cut (CCZ-HS) flow channel, and PFHS with a miniature circular pin-fin structure and inline arrangement (MCFHS) using nanofluids as coolants has never been seen in the existing literature. As a result, the aim of this work is to study the thermal and hydraulic performances of MCFHS and then to compare them with those of CCZ-HS using SiO_2-water nanofluids as coolants. Particle volume fractions of 0.2, 0.3, and 0.6 vol.% are used. Both heat sinks with a dimension of 28 × 33 mm are equally designed and tested.

2 Experimental apparatus and procedure

To evaluate and compare the thermal and hydraulic performances of heat sinks with a circular pin-fin structure and multiple-zigzag flow channel shape, an experimental setup is designed and built as schematically shown in Fig. 1. A nanofluid-cooled and water-cooled system are also tested under the same operating condition. With a focus on the test section, a comparison between PFHS with a miniature circular pin-fin and inline arrangement (MCFHS), and MCHS with a multiple-zigzag flow channel and single cross-cut (CCZ-HS) flow channel is conducted. MCFHS made of aluminum material is fabricated with a dimension of 28 × 33 mm. The dimension of the each circular fin is 1.2 mm in diameter and 1.2 mm in height. The total heat transfer area and hydraulic diameter of each flow channel are about 1430 mm^2 and 1.2 mm, respectively. Likewise, CCZ-HS is performed using copper material with a dimension of 28 × 33 mm and 1 mm in channel height. The hydraulic diameter of each flow channel and heat transfer area are 1 mm and 1238 mm^2, respectively. The cover plate is formed using acrylic material and is placed on the top of the heat sinks. The same cover plate dimension

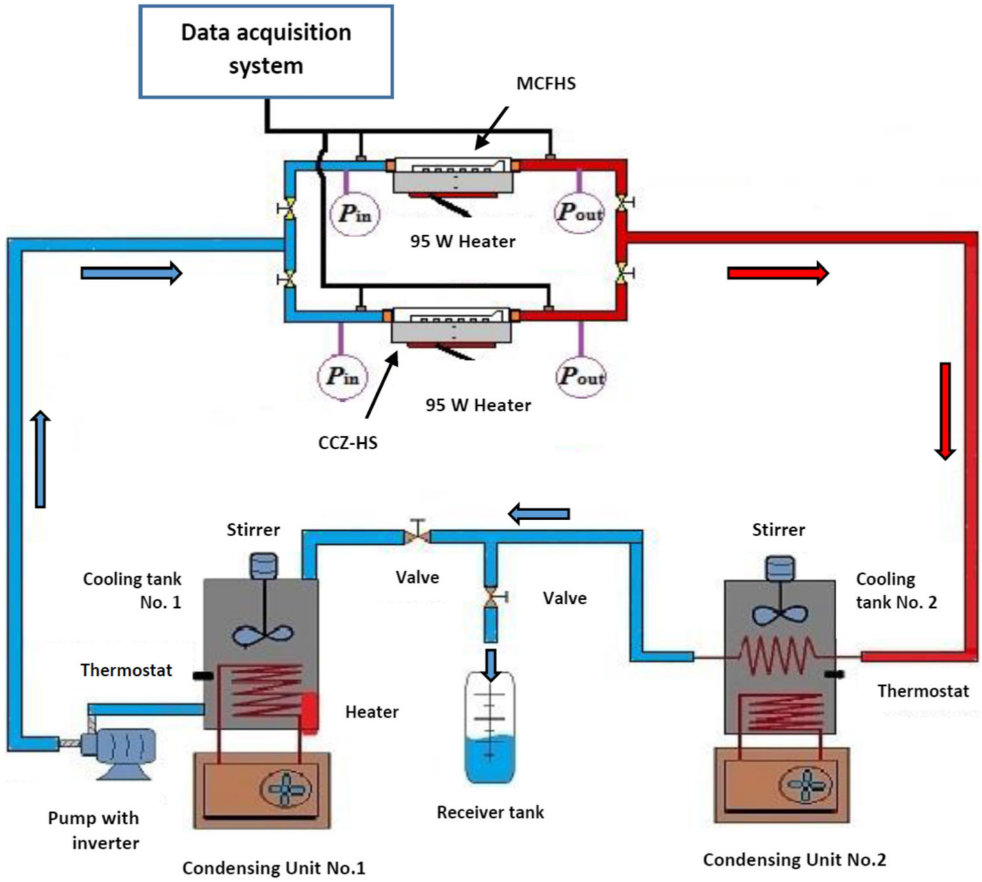

Fig. 1 Schematic diagram of the test loop used in this study

and configuration are used for MCFHS and CCZ-HS to avoid the effect of flow passage on the convective heat transfer and pressure drop data. Figure 2 and Table 1 show the configuration and main dimension of the MCFHS and CCZ-HS used in the present study. A 95-W electric heater is attached at the bottom side of each heat sink, and the supply heat load can be varied using a Variac transformer. Heat fluxes ranging from 10 to 60 kW/m^2 are adjusted. For the bulk fluid temperature measurement, T-Type sheath thermocouples are inserted into the center of the upstream and downstream tubes. To estimate the surface temperature of heat sinks, two positions of the T-type of thermocouples are drilled at 5 and 15 mm from the upper surface to record the temperature. Then, the surface temperature is estimated by means of linear extrapolation. Similarly, for the pressure drop measurement, two digital pressure gauges are positioned at the upstream and downstream side of each heat sink to measure the local pressure. For the mass flow rate measurement, a receiver tank is used to store the amount of discharge fluid per unit time. Five measurements are taken and then averaged. A pump with a speed controller is used to vary the flow rate of the test fluid. The uncertainty of all instruments is as follows: ±0.1 °C for the temperature, ±0.6 g for the weighting machine, and ± 50 Pa for the pressure measurement. To maintain a constant fluid temperature, two cooling tanks are used. Tank No. 1 with a cooling capacity of 3500 W is used to create the required temperature. Likewise, tank No.2 with the same cooling capacity is employed to reduce the fluid temperature that exits from the heat sink as the temperature of tank No. 1. This process is necessary to meet the steady-state condition during the test run. Finally, after the steady-state condition is achieved, all temperature and pressure measurements, along with the flow rate, are recorded.

To prepare the nanofluids, the two-step technique is employed. At present, this technique is most commonly used to produce nanofluids because various types of nanoparticles are commercially produced. This technique is more suitable for oxide nanoparticles. In this work, SiO_2 nanoparticles with a mean diameter of 15 nm are used, and deionized water is also used as the base fluid. The particle loadings are 0.2, 0.3, and 0.6 vol.%. First, SiO_2 nanopowders with desired particle concentrations are mixed with deionized water. Then, the solution is sonicated using an ultrasonic mixer with a power of 500 W continuously for 2 h. The ultrasonic mixer is usually required to intensively disperse and reduce the agglomeration of the nanoparticles. The thermal conductivity, true density, and specific heat of the SiO_2 nanoparticles are 1.37 W/m°C, 2648 kg/m^3, and 742 J/kg°C, respectively.

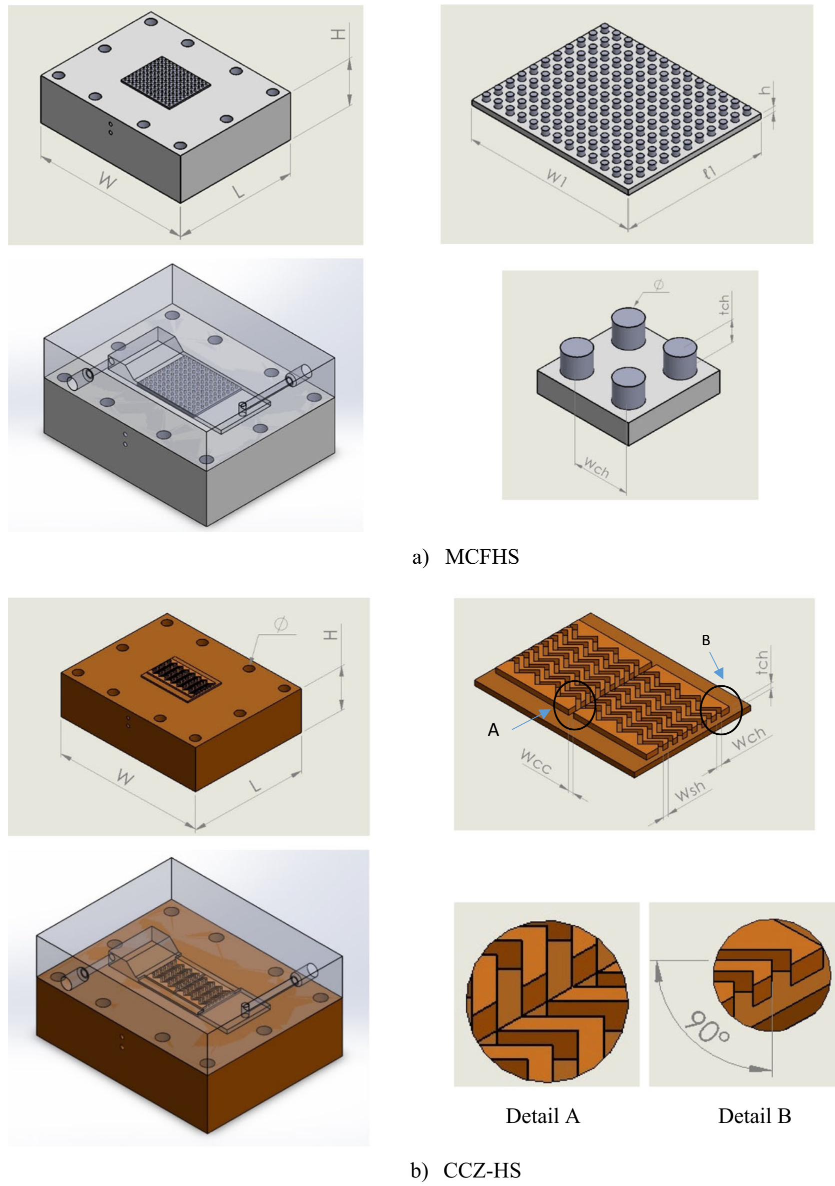

Fig. 2 The geometry and configuration of the heat sinks used in the present work

3 Calculation methodology

In the present work, the convective heat transfer and flow performances of MCFHS and CCZ-HS are studied and compared, both with a nanofluid-cooled and water-cooled system. The following equations are used and described in detail as shown in the below subsection.

To calculate the forced convective heat transfer coefficient, the following equations are necessary:

$$Q = mC_P(T_{out} - T_{in}) \tag{1}$$

$$h = \frac{Q}{A_{HS}(T_S - T_b)} \tag{2}$$

in which, h is the heat transfer coefficient, Q is the heat transfer rate, T_S is the surface temperature of the heat sink, T_b is the bulk temperature of the fluid, and A_{HS} is the heat transfer area.

As described in the experimental apparatus and procedure, the surface temperature (T_S) of the test section presented in Eq. (2) can be estimated using the following equation.

$$T_S = T_1 - \frac{y_1}{y_2}(T_2 - T_1) \tag{3}$$

in which, T_1 and T_2 are the heat sink temperature at 5 and 15 mm, respectively from the upper surface and are normally called the "temperature gradient", y_1 is the length from the top surface to T_1, and y_2 is the length from T_1 to T_2.

Table 1 Main dimensions of the heat sinks used in this work

Parameter	MCFHS	CCZ-HS
W	95 mm	
L	75 mm	
H	28 mm	
W_{hs}	1 mm	
W_1	33 mm	
l_1	28 mm	
h	1 mm	
t_{ch}	1 mm	
y_1	5 mm	
y_2	15 mm	
W_{ch}	1.2 mm	1 mm
d_{PF}	1.2 mm	–
w_{cc}	–	1 mm
A_{HS}	1430 mm^2	1238 mm^2
θ	–	90°

Thermal resistance is computed from Eq. (4).

$$R_{th} = \frac{T_S - T_b}{Q} \tag{4}$$

The pumping power can be calculated using Eq. (5) as follows:

$$W_{pp} = Q_v \Delta P \tag{5}$$

where R_{th} is the thermal resistance, W_{pp} is the pumping power, ΔP is the measured pressure drop across the heat sink, and Q_v is the volume flow rate of the fluid.

An important parameter to indicate the net benefit of the heat sink performance using the nanofluids cooled is the performance index (η). This term is the ratio between the heat transfer enhancement and the pressure drop ratio as described below:

$$\eta = \frac{h_{nf}/h_w}{\Delta P_{nf}/\Delta P_w} \tag{6}$$

It should be noted that the above equations can be used for water and nanofluids. However, in the case of nanofluids, important thermophysical properties, such as the density, specific heat, thermal conductivity, and viscosity, are calculated using the following equations.

The Pak and Cho [24] correlations are used to calculate the density and specific heat as described below:

$$\rho_{nf} = \phi \rho_p + (1-\phi)\rho_w \tag{7}$$

$$C\rho_{nf} = \phi C\rho_p + (1-\phi)C\rho_w \tag{8}$$

Similarly, the Hamilton and Crosser equation [25] for thermal conductivity and the Einstein model [26] for viscosity are expressed as below:

$$k_{nf} = \left[\frac{k_p + 2k_w - 2\phi(k_w - k_p)}{k_p + 2k_w + \phi(k_w - k_p)}\right] k_w \tag{9}$$

$$\mu_{nf} = (1 + 2.5\phi)\mu_w \tag{10}$$

where ϕ is the volume fraction of nanoparticles, Cp is the specific heat, ρ is the density, k is the thermal conductivity, μ is the viscosity and subscripts of nf, p, and w are nanofluid, nanoparticles, and water, respectively.

4 Results and discussion

In the present study, the effects of heat sink types (MCFHS and CCZ-HS), particle concentration and nanofluid flow rate on the thermal performance, pressure drop and performance index are presented and compared. The experimental results are divided into three categories i.e. thermal performance, pressure drop and performance index.

4.1 Thermal performance

The wall surface temperatures of the test section are used to calculate the convective heat transfer coefficient. The effects of the particle concentration and heat sink type on the wall surface temperature are also presented. As shown in Fig. 3, it is evident that the increasing of the wall heat flux leads to an increase in the surface temperature. Similarly, the wall temperature decreases as the particle concentration is increased. This is because the nanoparticles' presence in the base fluid increases the thermal properties as well as the energy exchange process compared to the common base fluid. Thus, a

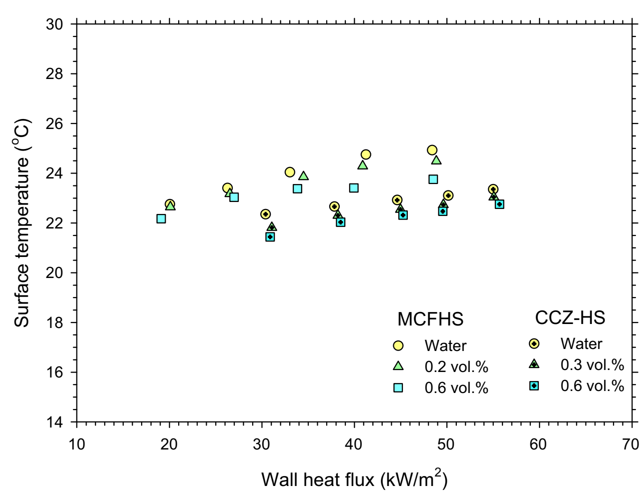

Fig. 3 Comparison of the surface temperature obtained from MCFHS and CCZ-HS

lower wall surface temperature is obtained. Moreover, Fig. 3 shows that the surface temperature of CCZ-HS is lower than that of MCFHS. Even though CCZ-HS has a lower heat transfer area than does MCFHS, a greater cooling performance is attained. This may be due to the fact that the effect of the channel diameter overcomes the effect of the heat transfer area. In the present study, the hydraulic diameter of CCZ-HS and MCFHS are 1 and 1.2 mm, respectively. This trend coincides well with the research work of Kandlikar and Grande [27]. They stated that a decrease in the channel diameter will lead to an increase in the heat transfer performance.

An important parameter commonly used to compare the thermal performance is the thermal resistance of the heat transfer devices as shown in Fig. 4a and b. A lower thermal resistance value means a greater cooling performance. Commonly, with all working fluids, the thermal resistance decreases with an increase in the mass flow rate or pumping power, as a higher fluid flow rate leads to an increase in the convective heat transfer performance. As expected, this behavior is obtained for the present study. Moreover, the effect of the heat sink configuration on the convective heat transfer coefficient is presented in Fig. 5. As described in Figs. 3 and 4, the measured data indicated that heat sinks with multiple-zigzag flow channels and single cross-cut (CCZ-HS) flow channels have greater thermal performances than do heat sinks with a miniature circular pin-fin structure (MCFHS). The surface temperature as well as the thermal resistance for CCZ-HS are obtained. As described above, although the heat transfer area of the CCZ-HS is smaller than that of the MCFHS, but the hydraulic diameter of the flow channel is also smaller, too. Thus, the effect of the channel diameter may be more dominant than the effect of the heat transfer area. For CCZ-HS, although the fluid flows pass the zigzag flow channel, a high level of turbulence of the main flow is created, which leads to an increase in the cooling performance. Moreover, a single cross-cut of the flow channel in the middle plan may lead to an increase in the turbulence intensity of the fluid flow at the same time. Thus, the convective heat transfer performance of CCZ-HS is about 24–55% higher than that of MCFHS. These results coincide well with the research work of Kim and Kim [9]. They reported that heat sinks with single cross-cut have superior heat transfer performance than do multiple cross-cut heat sinks. However, these results conflict with that of the research work of Shafeie et al. [1]. They identified that heat sinks with pin-fin structures have greater thermal performances than do microchannel heat sinks with simple straight flow channels. However, in their study, pin fins were located in a staggered arrangement, which normally has better thermal performance than does an inline arrangement as used in the present work. Moreover, a microchannel with a simple straight flow channel was used and compared. Therefore, the greater thermal performances of pin-fin heat sinks were obtained. For the present study, the miniature circular pin fins are

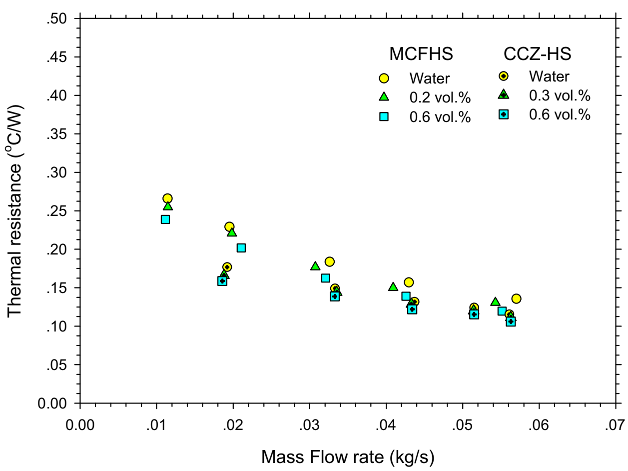

a) Thermal resistance VS mass flow rate

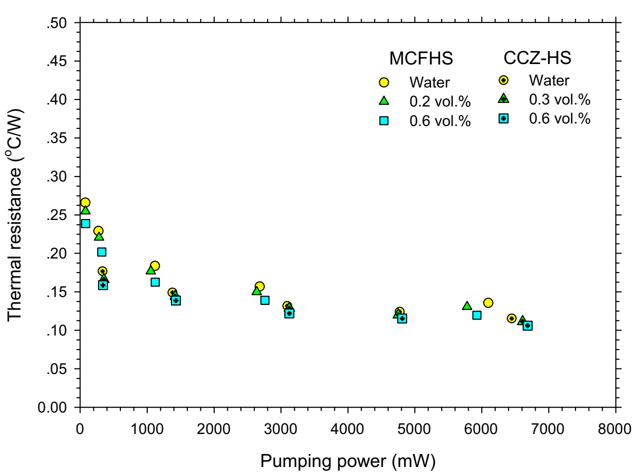

b) Thermal resistance VS pumping power

Fig. 4 Thermal resistance versus mass flow rate and pumping power at various particle fractions. **a** Thermal resistance VS mass flow rate (**b**) Thermal resistance VS pumping power

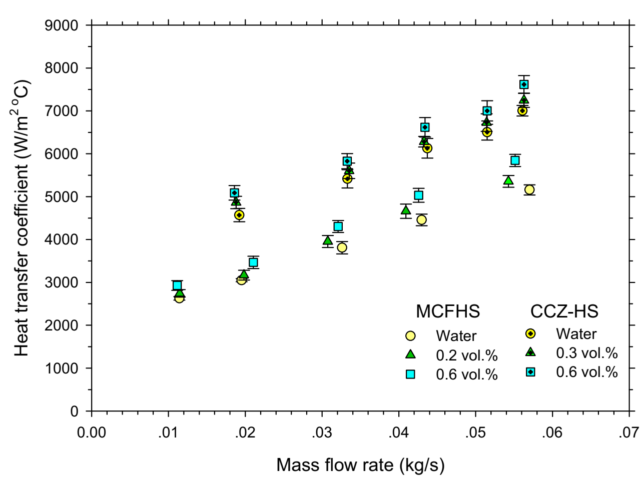

Fig. 5 Variation of the convective heat transfer coefficient as a function of system mass flow rate and heat sink types at different particle concentrations

placed in an inline arrangement, with the heat transfer performance of pin fins in the next row having the potential to deteriorate. Then, they are compared with MCHS with multiple-zigzag and single cross-cut flow channels. Thus, a lower heat transfer performance is obtained for MCFHS.

4.2 Pressure drop

The variation of the pressure drop across the test sections as a function of the particle concentration, heat sink type, and mass flow rate is demonstrated in Fig. 6. As expected, the pressure drop across the heat sink commonly increases with increasing the fluid flow rate. Moreover, it is confirmed that the presence of nanoparticles in the base fluid has a small effect on the pressure drop data. The pressure drop increases an average of only 3 to 4% for testing conditions as shown in Fig. 7. This is the advantage of the use of nanofluids as coolants: It enhances the heat transfer performance but creates little or no penalty drop in the pressure and pumping power. Moreover, from the present work, it is evident that the pressure drop of CCZ-HS is a few percentage points higher than that of MCFHS compared to the increase of the heat transfer enhancement. This means using the heat sink with a multiple-zigzag flow channel and single cross-cut flow channel gives higher thermal performances than does using the circular pin-fin heat sink with an inline arrangement.

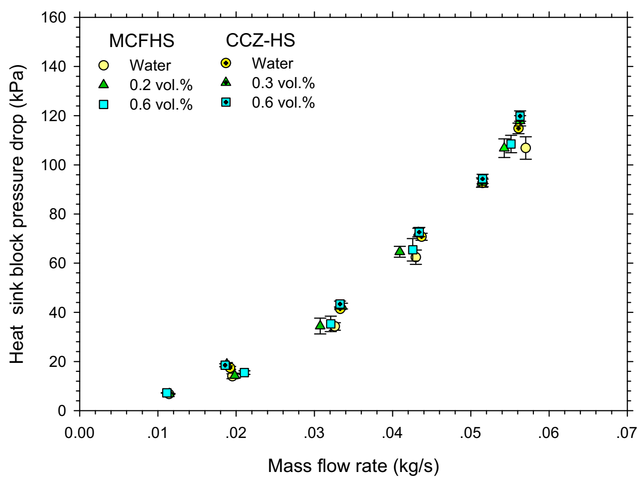

a) Pressure drop related with the mass flow rate

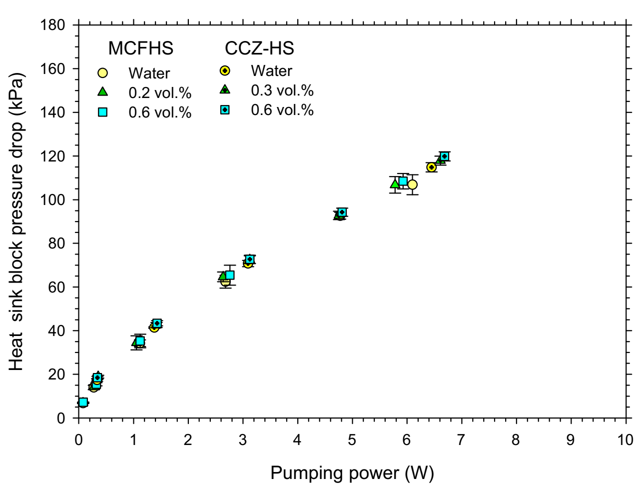

b) Pressure drop related with the pumping power

Fig. 6 Pressure drop versus mass flow rate for MCFHS and CCZ-HS. **a** Pressure drop related with the mass flow rate (**b**) Pressure drop related with the pumping power

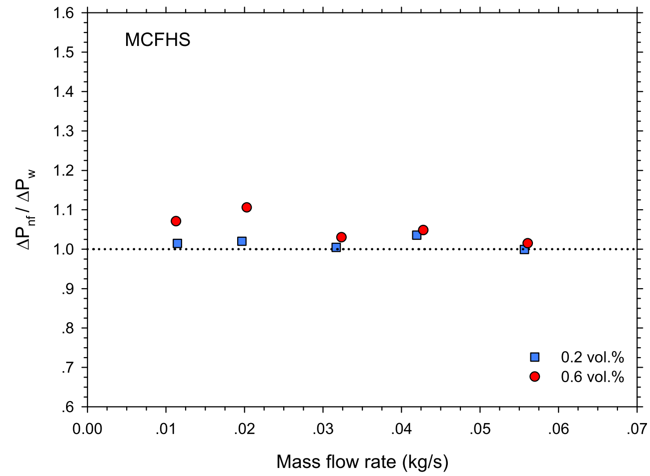

a) MCFHS

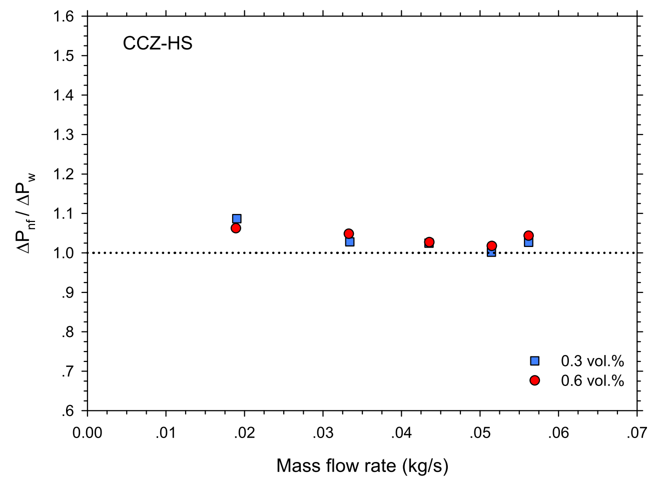

b) CCZ-HS

Fig. 7 Pressure drop ratio obtained from MCFHS and CCZ-HS as a function of particle concentrations (**a**) MCFHS (**b**) CCZ-HS

4.3 Performance index

The performance index, η described in Eq. (6) is plotted and shown in Fig. 8. For the value of η over 1, this means that the heat transfer enhancement by using nanofluids as coolants is greater than the pressure drop caused by the nanofluids. From the whole range of the experiment, it is clearly seen that most of the η values are over 1 and increase as the particle

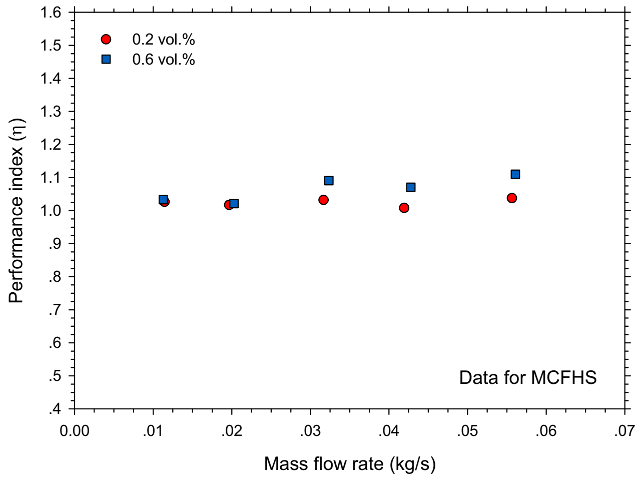

a) Data for MCFHS

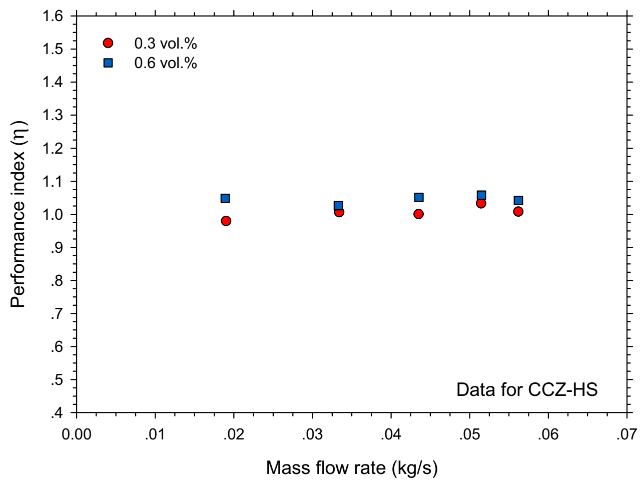

b) Data for CCZ-HS

Fig. 8 Performance index VS mass flow rate obtained from MCFHS and CCZ-HS. **a** Data for MCFHS (**b**) Data for CCZ-HS

concentration is increased, for both MCFHS and CCZ-HS. This behavior implies that using a nanofluid-cooled heat sink provides better cooling performance than does using a water-cooled heat sink. This is because nanofluids give better heat transfer performance but a small increase or no impact on the pressure loss.

5 Conclusions

In this study, an experimental investigation of the forced convective heat transfer, pressure drop, and performance index of two different types of heat sinks cooled by nanofluids is conducted. A heat sink with a miniature circular pin-fin arrangement and a heat sink with a multiple-zigzag flow channel and single cross-cut flow channel are compared. SiO_2 nanoparticles dispersed in water with particle fractions of 0.2, 0.3, and 0.6 vol.% are used. The important findings are summarized as follows:

1. Under testing conditions, the surface temperature increases with an increasing heat flux and decreases as the particle concentration increases.
2. The performance index of nanofluid-cooled heat sinks is significantly higher than those of water-cooled heat sinks.
3. A heat sink with a multiple-zigzag flow channel and single cross-cut (CCZ-HS) flow channel has superior cooling performance than does a heat sink with a miniature pin-fin inline arrangement (MCFHS) by around 24–55%. The effect of the channel diameter and channel configuration may overcome the effect of the heat transfer area.
4. The pressure drop of CCZ-HS is few percentage points greater than that of MCFHS.
5. In general, the thermal performance of the system is better but this advantage is obtained on the expenses of the high pumping power.

Acknowledgments The first author would like to thank the office of research of the Southeast Asia University (SAU) and the Thailand Research Fund (TRF). The second author acknowledges the support provided by the "Research Chair Grant" National Science and Technology Development Agency (NSTDA), and King Mongkut's University of Technology Thonburi through the "KMUTT 55th Anniversary Commemorative Fund".

References

1. Shafeie H, Abouali O, Jafarpur K, Ahmadi G (2013) Numerical study of heat transfer performance of single-phase heat sinks with micro pin-fin structures. Appl Therm Eng 58:68–76
2. Tuckerman DB, Pease RFW (1981) High performance heat sinking for VLSI. IEEE Electron Device Lett 2(5):126–129
3. Choi SUS (1995) Enhancing thermal conductivity of fluids with nanoparticle. ASME Fluids Eng Div 231:99–105
4. Duangthongsuk W, Wongwises S (2015) An experimental study on the thermal and hydraulic performances of nanofluids flow in a miniature circular pin fin heat sink. Exp Thermal Fluid Sci 66:28–35
5. Duangthongsuk W, Wongwises S (2015) Heat transfer and pressure drop in a pin fin heat sink using nanofluids as coolant. Adv Mater Res 1105:253–258
6. Duangthongsuk W, Wongwises S (2015) A comparison of the heat transfer performance and pressure drop of nanofluid-cooled heat sinks with different miniature pin fin configurations. Exp Thermal Fluid Sci 68:111–118
7. Kim SJ, Kim DK, Oh HH (2008) Comparison of fluid flow and thermal characteristics of plate-fin and pin-fin heat sinks subject to a parallel flow. Heat Transfer Eng 29(2):169–177
8. Yang YT, Peng HS (2009) Numerical study of thermal and hydraulic performance of compound heat sink. J Num Heat Transfer Part A Appl 55(5):432–447

9. Kim TY, Kim SJ (2009) Fluid flow and heat transfer characteristics of cross-cut heat sinks. Int J Heat Mass Transf 52:5358–5370
10. Teja VS, Ramakrishna A, Rao R (2014) Numerical study of different cross-sectional stacked microchannel heat sink. Int J Eng Res Technol 3:54–59
11. Jang SP, Choi SUS (2006) Cooling performance of a microchannel heat sink with nanofluids. Appl Therm Eng 26:2457–2463
12. Lee J, Mudawar I (2007) Assessment of the effectiveness of nanofluids for single-phase and two-phase heat transfer in microchannels. Int J Heat Mass Transf 50:452–463
13. Bhattacharya P, Samanta AN, Chakraborty S (2009) Numerical study of conjugate heat transfer in rectangular microchannel heat sink with Al_2O_3/H_2O nanofluid. Heat Mass Transf 45(10):1323–1333
14. Li J, Kleinstreuer C (2008) Thermal performance of Nanofluid flow in microchannels. Int J Heat Fluid Flow 29:1221–1232
15. Ho CJ, Wei LC, Li ZW (2010) An experimental investigation of forced convective cooling performance of a microchannel heat sink with Al_2O_3/water nanofluid. Appl Therm Eng 30:96–103
16. Lelea D (2011) The performance evaluation of Al_2O_3/water nanofluid flow and heat transfer in microchannel heat sink. Int J Heat Mass Transf 54:3891–3899
17. Mohammed HA, Bhaskaran G, Shuaib NH, Abu-Mulaweh HI (2011) Influence of nanofluids on parallel flow square microchannel heat exchanger performance. Int Commun Heat Mass Transfer 38(1):1–9
18. Selvakumar P, Suresh S (2012) Convective performance of CuO/water nanofluid in an electronic heat sink. Exp Thermal Fluid Sci 40:57–63
19. Hung TC, Yan WM, Wang XD, Chang CY (2012) Heat transfer enhancement in microchannel heat sinks using nanofluids. Int J Heat Mass Transf 55(9–10):2559–2570
20. Putra N, Septiadi WN, Julian G, Maulana A, Irwansyah R (2013) An experimental study on thermal performance of nano fluids in microchannel heat exchanger. Int J Technol 2:167–177
21. Wu J, Zhao J, Lei J Liu B (2016) Effectiveness of nanofluid on improving the performance of microchannel heat sink. Appl Thermal Eng 101:402–412
22. Azizi Z, Alamdari A, Malayeri MR (2016) Thermal performance and friction factor of a cylindrical microchannel heat sink cooled by cu-water nanofluid. Appl Therm Eng 99:970–978
23. Duangthongsuk W, Wongwises S (2017) An experimental investigation on the heat transfer and pressure drop characteristics of nanofluid flowing in microchannel heat sink with multiple zigzag flow channel structures. Exp Thermal Fluid Sci 87:30–39
24. Pak BC, Cho YI (1998) Hydrodynamic and heat transfer study of dispersed fluids with submicron metallic oxide particles. Exp Heat Transfer 11:151–170
25. Hamilton RL, Crosser OK (1962) Thermal conductivity of heterogeneous two-component systems. Ind Eng Chem Fundam 1(3): 187–191
26. Drew DA, Passman SL (1999) Theory of multi component fluids. Springer, Berlin
27. Kandlikar SG, Grande WJ (2003) Evolution of microchannel flow passages – Thermohydraulic performance and fabrication technology. Heat Transfer Eng 24(1):3–17